DALTON
FULL PAPER

# Rhodium and iridium complexes with thiolate and tertiary phosphine ligands. The synthesis and structures of *trans*-$[Ir(SC_6H_3Cl_2\text{-}2,6)(CO)(PPh_3)_2]$, $[Rh_2(\mu\text{-}SC_6H_3Pr^i_3\text{-}2,4,6)_2(CO)_2(PPh_3)_2]$, $[Rh_2H_2(\mu\text{-}SC_6H_4PPh_2\text{-}2)_2(CO)_2(PPh_3)_2][BF_4]_2$, and $[Rh_2I_6(MeSC_6H_4PPh_2\text{-}2)_2]$

**Jonathan R. Dilworth,* David Morales and Yifan Zheng**

*Inorganic Chemistry Laboratory, University of Oxford, South Parks Road, Oxford, UK OX1 3QR*

***Received 18th February 2000, Accepted 19th July 2000***
***Published on the Web 14th August 2000***

Reaction of $[MF(CO)(PPh_3)_2]$ (M = Rh or Ir) with bulky aromatic thiols ArSH gave the binuclear complexes $[M_2(\mu\text{-}SAr)_2(CO)_2(PPh_3)_2]$ (M = Rh, SAr = $SC_6H_2Pr^i_3$-2,4,6 or $SC_6H_3Me_2$-2,6) and mononuclear complexes $[M(SAr)(CO)(PPh_3)_2]$ (M = Rh or Ir, SAr = $SC_6H_3Cl_2$-2,6 or $SC_6H_4SiPh_3$-2; M = Ir, SAr = $SC_6H_2Pr^i_3$-2,4,6 or $SC_6H_3Me_2$-2,6. The crystal structure of $[Rh_2(\mu\text{-}SC_6H_3Pr^i_3\text{-}2,4,6)_2(CO)_2(PPh_3)_2]$ showed a binuclear thiolate bridged core while that of $[Ir(SC_6H_3Cl_2\text{-}2,6)(CO)(PPh_3)_2]$ revealed a conventional square planar geometry with *trans* $PPh_3$ ligands. Three rhodium complexes were shown to be efficient catalysts for the hydroformylation of hept-1-ene under mild conditions with good selectivity for linear aldehyde for SAr = $SC_6H_4SiPh_3$-2. Reaction of $[MF(CO)(PPh_3)_2]$ with phosphinothiolate proligands PSH gave the monomeric complexes $[M(PS)(CO)(PPh_3)_2]$ (M = Rh or Ir; PS = $SC_6H_4PPh_2$-2 or $S(CH_2)_3PPh_2$; M = Rh, PS = $SCH_2CH_2PPh_2$ or $SCH(CH_3)CH_2PPh_2$). The complex $[Rh(SC_6H_4PPh_2\text{-}2)(CO)(PPh_3)]$ reacted reversibly with protons ($HBF_4$) to give the dimeric dication $[Rh_2(\mu\text{-}SC_6H_4PPh_2\text{-}2)_2(CO)_2(PPh_3)_2]^{2+}$, shown by a crystal structure be a thiolate bridged dimer with an Rh–Rh bond and pseudo-octahedral geometry about each $Rh^{III}$. Electrophilic attack by $[Me_3O][BF_4]$ on $[Rh(SC_6H_4PPh_2\text{-}2)(CO)(PPh_3)]$ occurred at sulfur to give $[Rh(MeSC_6H_4PPh_2\text{-}2)(CO)(PPh_3)]^+$ and excess of MeI gave $[Rh_2I_6(MeSC_6H_4PPh_2\text{-}2)_2]$, with octahedral $Rh^{III}$ linked by a double iodide bridge. Attack at sulfur also occurred in $[Rh(SC_6H_4PPh_2\text{-}2)(CO)(PPh_3)]$ with $I(CH_2)_3I$ and $ICH_2CO_2H$ to give $[Rh(2\text{-}Ph_2PC_6H_4SCH_2CH_2CH_2)(CO)(PPh_3)]$ and $[RhI_2(2\text{-}Ph_2PC_6H_4SCH_2CO_2)(PPh_3)]$ respectively. The complex $[RhI_3(CO)(PPh_3)_2]$ was a by-product and shown by a crystal structure to have a pseudo-octahedral structure with *trans*-$PPh_3$ ligands.

## Introduction

Although thiolate complexes of $Rh^I$ and $Ir^I$ with tertiary phosphine co-ligands are well documented, the majority are polynuclear with bridging thiolates[1] and examples of mononuclear complexes are rare. A wide range of binuclear complexes containing simple di-μ-thiolate bridges are known, and $[Ir_2(\mu\text{-}SCMe_3)_2(CO)_2(P(OMe)_3)_2]$ is typical. The tridentate trithiol $CH_3C(CH_2SH)_3$ forms trinuclear thiolate bridged complexes of the type $[CH_3C\{CH_2SRh(CO)(P(OMe)_3)\}_3]$.[2] In addition many complexes with mixed bridging ligand systems are also known and exemplified by $[Ir_2(\mu\text{-}pz)(\mu\text{-}SCMe_3)(CO)_2(P(OMe_3)_2)_2]$.[3]

The chemistry of rhodium and iridium complexes with hybrid phosphorus–sulfur donor chelating ligands is by comparison less well explored.[4] However such ligands appear to bind very effectively to platinum group metals, and complexes with $Rh^I$ have been shown to be robust and efficient catalysts for the carbonylation of methanol.[5,6] The thiolate-bridged dimeric complexes $[Rh_2(PS)_2(CO)_2]$ (PS = $Ph_2PCH_2CH_2S$, $Ph_2PC_6H_{10}S$ or $Ph_2PC_6H_4S$-2) and $[M_2(Ph_2PC_6H_4S\text{-}2)(COD)_2]$ (M = Rh or Ir; COD = cyclooctadiene) have been known for some time.[5] Recently the synthesis of the monomeric complexes $[M(Ph_2PC_6H_4S\text{-}2)(CO)(PPh_3)]$ (M = Rh or Ir) was also reported,[7] together with the chemistry of the alkoxide analogues. The PS ligands with aliphatic backbones behave differently, and reaction of $[IrCl(CO)(PPh_3)_2]$ with 2 equivalents of $Ph_2PCH_2CH_2SH$ in the presence of base generated the iridium(III) complex $[IrH(Ph_2PC_6H_4S)_2(CO)]$.[8] The binucleating phosphinothiol proligand $HSC_6H_3(CH_2PPh_2)_2$-2,6 (PSHP) reacts with $[MCl(CO)(PPh_3)_2]$ (M = Rh or Ir) to give $[Rh_2Cl(PSP)(CO)_2]$ (with half an equivalent of PSHP) and $[Ir_2Cl_2(PSP)_2(\mu\text{-}CO)]$[9] (with one equivalent).

The oxidative addition chemistry of dinuclear thiolate bridged complexes of rhodium and iridium has been studied in some detail. Depending on the binuclear complex used as the starting point, bifunctional agents such as diiodomethane react to give complexes with triple bridges comprising a methylene group and two thiolate sulfurs or a methylene with one bridging thiolate sulfur and another bridging ligand such as pyrazole.[10,11] Dimethyl acetylene dicarboxylate oxidatively adds to give species such as $[Ir_2(\mu\text{-}pz)(\mu\text{-}SBu^t)(\mu\text{-}MeO_2CC{=}CCO_2Me)(CO)_2(P(OMe)_3)_2]$ with a triple bridge including the acetylene molecule, bonded as a dimetallated olefin.[2] In contrast, tetracyanoethylene adds in asymmetric fashion to $[Ir_2(\mu\text{-}SBu^t)_2(CO)_2(PR_3)_2]$ (R=Me, Ph or OMe) to give the complexes $[(RP_3)_2(OC)Ir(\mu\text{-}SBu^t)_2Ir(CO)(C_2(CN)_4)]$.[12] Significant rearrangement also occurs on addition of hexafluoro-2-butyne to $[Ir_2(\mu\text{-}SBu^t)_2(CO)_4]$ to give trinuclear 'crown-like' complexes of the type $[Ir_3(\mu\text{-}SBu^t)_3(\mu\text{-}C_4F_6)(CO)_6]$.[13]

In view of the comparative paucity of data on mononuclear complexes we have investigated the synthesis and reactivities of complexes of the type $[Ir(SAr)(CO)(PPh_3)_2]$ (M = Rh or Ir; Ar = 2,6-disubstituted arene) and $[Rh(Ph_2PC_6H_4S\text{-}2)(CO)(PPh_3)]$. The presence of thiolate ligands in such complexes introduces the possibility of chemistry occurring at sulfur and

**Table 1** Complexes of rhodium(I) and iridium(I) with bulky aromatic thiolates

| Complex | Colour | Elemental analysis (%)[a] C | H | $\tilde{\nu}$(CO)[b] | NMR ($\delta$, $J$/Hz)[c] $^{31}$P | $^{1}$H | MS[d] ($m/z$) |
|---|---|---|---|---|---|---|---|
| **1** *trans*-[Rh(DCBT)(CO)($PPh_3$)$_2$] | Yellow | 60.0 (60.0) | 3.9 (4.0) | 1965 | 32.2 (d), $J_{P\text{-}Rh}$ = 133.4 | 7.1–7.8 (m) (33 H, aromatic) | 804 $(M - CO)^+$ |
| **2** *trans*-[Rh(TPSBT)(CO)($PPh_3$)$_2$] | Yellow | 70.8 (71.6) | 4.8 (4.8) | 1978 | 30.50 (d), $J_{P\text{-}Rh}$ = 133.6 | 6.8–7.8 (m) (49 H, aromatic) | 1022 ($M^+$) |
| **3** [$Rh_2$(μ-DMBT)$_2$(CO)$_2$($PPh_3$)$_2$] | Yellow | 60.2 (60.9) | 3.9 (4.0) | 1966 | 34.2 (d), $J_{P\text{-}Rh}$ = 156.7 | 6.5–7.5 (m) (36 H, aromatic), 2.74(s) (6 H, $CH_3$), 1.54(s) (6 H, $CH_3$) | 1060 $M^+$ |
| **4** [$Rh_2$(μ-TIPBT)$_2$(CO)$_2$($PPh_3$)$_2$] | Yellow | 64.5 (65.0) | 6.0 (6.1) | 1976 | 35.0 (d), $^1J_{P\text{-}Rh}$ = 153.6 | 6.6–7.7 (m) (34 H, aromatic), 5.6 (m), 4.8 (m), 4.3 (m), 2.7 (m) (4 H, CH), 0.6–1.6 (m) (36 H, $CH_3$) | 1229 $(M + 1 - CO)^+$ |
| **5** *trans*-[Ir(DCBT)(CO)($PPh_3$)$_2$] | Yellow | 55.7 (56.9) | 3.6 (3.6) | 1946 | 20.8(s) | 6.7–7.8 (m) (33 H, aromatic) | 945 $(M + Na)^+$ |
| **6** *trans*-[Ir(TPSBT)(CO)($PPh_3$)$_2$] | Yellow | 66.0 (65.9) | 4.4 (4.4) | 2004 | −3.4(s) | 6.4–7.7 (m) (49 H, aromatic) | 1111 ($M^+$) |
| **7** *trans*-[Ir(DMBT)(CO)($PPh_3$)$_2$] | Yellow | 63.7 (63.7) | 4.4 (4.5) | 2035 | 9.31(s) | 6.8–7.9 (m) (33 H, aromatic), 2.3(s) (6 H, $CH_3$) | 853 $(M - CO)^+$ |
| **8** *trans*-[Ir(TIPBT)(CO)($PPh_3$)$_2$] | Yellow | 61.2 (61.3) | 4.4 (4.5) | 2035 | 9.21(s) | 6.8–7.9 (m) (32 H, aromatic), 2.6–3.7 (m) (3 H, CH), 0.6–14 (m) (18 H, $CH_3$) | 951 $(M - CO)^+$ |

[a] Calculated values in parentheses. [b] As Nujol mulls, in $cm^{-1}$. [c] In $CDCl_3$ solution. [d] FAB mass spectra in 3-nitrobenzyl alcohol matrix.

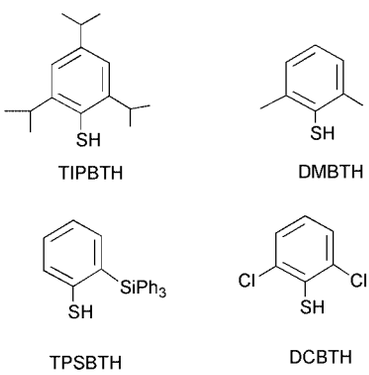


**Fig. 1** Structures and abbreviations of aromatic thiol proligands.

we have explored the balance between electrophilic attack at the metal and sulfur.

## Results and discussion

### Synthesis of complexes of sterically hindered thiolates

Reaction of [RhCl(CO)($PPh_3$)$_2$] with free thiols RSH gives oxidation addition products and with sodium or lithium salts complex mixtures can be formed. However [RhF(CO)($PPh_3$)$_2$] with bulky aromatic thiols in toluene gives the complexes [M(SAr)(CO)($PPh_3$)$_2$] (M = Rh, SAr = DCBT (**1**) or TPSBT (**2**); M = Ir, SAr = DCBT (**5**), TPSBT (**6**), DMBT (**7**) or TIPBT (**8**)) and [$Rh_2$(μ-SAr)$_2$(CO)$_2$($PPh_3$)$_2$] (SAr = TIPTB (**4**) or DMBT (**3**)). The structures and abbreviations for the thiols are summarised in Fig. 1, and the syntheses are summarised in Scheme 1. The complexes were isolated as moderately air-stable bright yellow solids, and analytical and spectroscopic data are summarised in Table 1.

The spectroscopic properties of the monomeric complexes were generally entirely consistent with a planar structure. Two thiols DCBTH and TIPBTH gave dimeric complexes with Rh, reflecting the greater steric constraints exerted by the 2,6-isopropyl or 2,6-chloro substituents, which cause loss of a triphenylphosphine ligand. The greater kinetic stability of iridium leads to monomeric iridium(I) complexes as triphenylphosphine is not lost. The $^1$H NMR of complex **7** indicates that both Me groups are equivalent, indicating a symmetrical

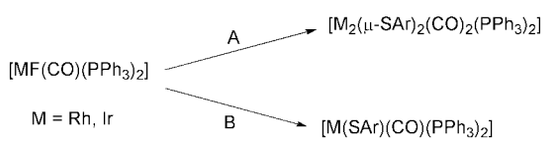


A: Reaction with ArSH, M = Rh, SAr = TIPBT, DMBT

B: Reaction with ArSH, M = Rh, Ir, ArS = DCBT, TPSBT
M = Ir, SAr = TIPBT, DMBT

**Scheme 1** Synthesis of thiolate complexes of $Ir^I$ and $Rh^I$.

disposition of the aromatic thiolate groups. In the dimeric rhodium complex **3** the two thiolates are presumably equivalent in the *anti* configuration (see structure of **4** below), but the Me groups are inequivalent, and appear as two singlets. For the rhodium complexes **1** and **2** the Rh–P coupling constants of *ca.* 134 Hz are consistent with a *trans* arrangement of the tertiary phosphine ligands.

### The crystal and molecular structure of [$Rh_2$(μ-TIPBT)$_2$(CO)$_2$($PPh_3$)$_2$] 4

A ZORTEP[14] representation of the structure appears in Fig. 2 and selected bond lengths and angles are shown in Table 2. The two square planar rhodium(I) units are bridged by two arenethiolate sulfurs with the arene groups adopting an *anti* arrangement with respect to the $Rh_2S_2$ core. The observation of only two singlets in the $^1$H NMR of the DMTB analogue suggests free rotation about the C–S bond in solution. The Rh–S distances are very similar to those observed for *anti*-[$Rh_2$(μ-$SBu^t$)$_2$(CO)$_2$($PPh_3$)$_2$][15] (2.357(1) and 2.391(6) Å) and [$Rh_2$(μ-SPh)$_2$(CO)$_2$($PPh_3$)$_2$][16] (2.375(7) and 2.400(7) Å). The slightly longer Rh–S distances observed in **4** are ascribable to the steric effects exerted by the 2,6-substituents in the arenethiolate group. The $Rh_2S_2$ has a characteristic 'butterfly' configuration and the Rh···Rh distance of 3.522(1) Å indicates the absence of a Rh–Rh bond.

### The crystal and molecular structure of [Ir(DCBT)(CO)($PPh_3$)$_2$] 5

A ZORTEP representation of the molecular structure of complex **5** is shown in Fig. 3, and selected bond lengths and angles are shown in Table 3. The geometry about iridium is slightly

**Table 2** Selected bond lengths (Å) and angles (°) for compound **4**

| | | | |
|---|---|---|---|
| Rh(1)–C | 1.764(8) | S(2)–C(21) | 1.803(7) |
| Rh(1)–P(1) | 2.266(2) | P(1)–C(41) | 1.813(7) |
| Rh(1)–S(1) | 2.369(2) | P(1)–C(61) | 1.813(8) |
| Rh(1)–S(2) | 2.415(2) | P(1)–C(52) | 1.876(7) |
| Rh(2)–C(0) | 1.814(8) | P(2)–C(31) | 1.812(7) |
| Rh(2)–P(2) | 2.267(2) | P(2)–C(81) | 1.842(7) |
| Rh(2)–S(1) | 2.368(2) | P(2)–C(71) | 1.851(8) |
| Rh(2)–S(2) | 2.448(2) | C–O | 1.217(8) |
| S(1)–C(11) | 1.798(7) | C(0)–O(0) | 1.150(9) |
| | | | |
| C–Rh(1)–P(1) | 92.1(2) | P(2)–Rh(2)–S(2) | 96.65(7) |
| C–Rh(1)–S(1) | 93.5(2) | S(1)–Rh(2)–S(2) | 80.76(6) |
| P(1)–Rh(1)–S(1) | 169.90(7) | C(11)–S(1)–Rh(1) | 116.2(2) |
| C–Rh(1)–S(2) | 171.1(2) | C(11)–S(1)–Rh(2) | 114.1(2) |
| P(1)–Rh(1)–S(2) | 94.03(7) | Rh(1)–S(1)–Rh(2) | 96.05(7) |
| S(1)–Rh(1)–S(2) | 81.45(6) | C(21)–S(2)–Rh(1) | 119.1(2) |
| C(0)–Rh(2)–P(2) | 89.9(2) | C(21)–S(2)–Rh(2) | 117.7(3) |
| C(0)–Rh(2)–S(1) | 92.7(2) | Rh(1)–S(2)–Rh(2) | 92.81(6) |
| P(2)–Rh(2)–S(1) | 170.69(7) | O–C–Rh(1) | 177.1(6) |
| C(0)–Rh(2)–S(2) | 173.4(2) | O(0)–C(0)–Rh(2) | 177.3(8) |

**Table 3** Selected bond lengths (Å) and angles (°) for compound **5**

| | | | |
|---|---|---|---|
| Ir–C | 1.824(4) | P(2)–C(41) | 1.833(3) |
| Ir–P(2) | 2.3238(9) | P(2)–C(61) | 1.835(3) |
| Ir–P(1) | 2.3335(8) | S(3)–C(71) | 1.756(4) |
| Ir–S(3) | 2.3933(9) | Cl(1)–C(72) | 1.737(5) |
| P(1)–C(21) | 1.828(3) | Cl(2)–C(76) | 1.733(6) |
| P(1)–C(11) | 1.827(3) | O–C | 1.153(5) |
| P(2)–C(51) | 1.824(3) | | |
| | | | |
| C–Ir–P(2) | 92.25(11) | P(2)–Ir–S(3) | 85.66(3) |
| C–Ir–P(1) | 86.42(11) | P(1)–Ir–S(3) | 94.68(3) |
| P(2)–Ir–P(1) | 174.31(3) | O–C–Ir | 177.0(3) |
| C–Ir–S(3) | 169.67(12) | | |

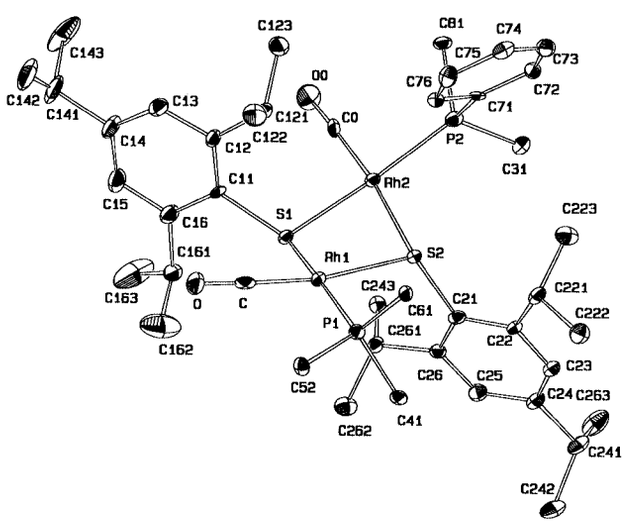


**Fig. 2** A ZORTEP representation of the structure of $[Rh_2(\mu\text{-TIPBT})_2(CO)_2(PPh_3)_2]$ **4** showing the atom labelling scheme. The tertiary phosphine phenyl groups are omitted for clarity.

distorted square planar with C–Ir–P(2) 92.25(11), C–Ir–P(1) 86.42(11)°, P(2)–Ir–S(3) 85.67(5)° and P(1)–Ir–S(3) 94.68(3). The orientation of the DCBT ligand is such as to bring one Cl substituent close to the metal with an Ir···Cl(1) distance of 3.197(1) Å. This suggests weak donation of electron density of the Cl lone pairs to the iridium, which may explain the lower value for $\nu$(CO) for this complex compared to those of the other monomeric iridium(I) complexes. The Ir–S bond length of 2.393(2) Å is somewhat longer than that observed for other monomeric thiolate complexes such as $[Ir(\eta^5\text{-}C_5Me_5)(SC_6F_4H)_2]$.[16] However the variations in ligands and oxidation states make a precise comparison difficult.

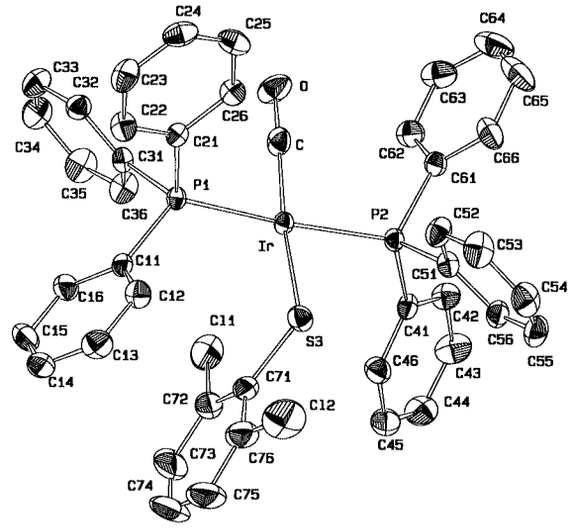


**Fig. 3** A ZORTEP representation of the structure of $[Ir(DCBT)(CO)(PPh_3)_2]$ **5** showing the atom labelling scheme.

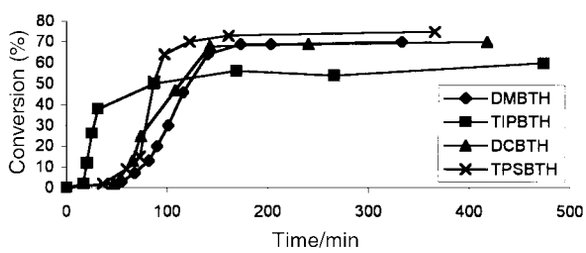


**Fig. 4** Percentage conversion of olefin into linear aldehyde for the hydroformylation of 1-heptene (70 °C, 5 bar forming gas) for a range of rhodium(I) aromatic thiolate complexes.

## Catalytic activity of rhodium thiolate complexes

The catalytic activity of binuclear complexes such as $[Rh_2(\mu\text{-}SR)_2(CO)_2P_2]$ (R = $Bu^t$ or $Me_2NCH_2CH_2$, P = tertiary phosphine), particularly for hydroformylation or aminomethylation, has been explored in some detail.[18–20] *In situ* IR experiments showed the formation of mononuclear hydrides such as $[RhHP_3]$ under hydroformylation conditions (80 °C, 5–30 bar). Deuterioformylation experiments provided no evidence for the involvement of binuclear species.[21] Similar results were obtained in water using sulfonated triphenylphosphine to confer solubility.[22] Generally conversion rates are reasonably high and use of chiral diphosphines provides high regioselectivity and medium to high enantiomeric excesses.[23] Asymmetric hydroformylation of styrene has also been achieved using 1,1′-binaphthalene-2,2′-dithiol complexes of $Rh^I$.[24]

Here both monomeric and dimeric rhodium complexes **1**, **2** and **4** were tested for hydroformylation catalysis activity for 1-heptene, and the results are presented in Fig. 4. High conversion rates are obtained under the mild conditions (70 °C, 5 bar forming gas) with reasonable to good regioselectivities for formation of linear as opposed to branched aldehydes. Maximum selectivity for linear aldehyde was observed for complex **2** of the asymmetrically substituted thiol TPSBTH where the single large $Ph_3Si$ group is clearly able to exert steric influence on the reaction stereochemistry at the olefin insertion step. There is no discernible difference in rate or selectivity between the dimeric and monomeric complexes and in view of the results obtained above it seems likely that both give rise to monomeric intermediates. The overall conversion rates are comparable with those for $[RhCl(PPh_3)_3]$ and the selectivity to linear aldehyde formation is approximately twice that for Wilkinson's complex. The strong dependence of conversion yield and stereochemistry on the thiolate suggests that thiolate

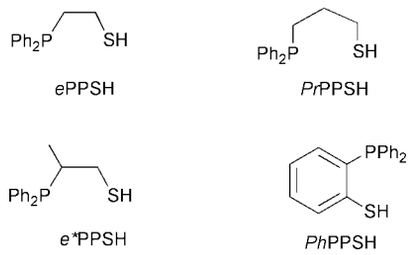


**Fig. 5** Structures and abbreviations for phosphinothiol proligands.

co-ordination may be retained in the active catalyst under the conditions used, although involvement as a non-co-ordinated anion cannot be excluded.

### Synthesis of phosphinothiolate complexes

We describe here the convenient high yield (*ca.* 90%) syntheses of complexes of the type $[M(PS)(CO)(PPh_3)_2]$ **9**–**14** (M = Rh or Ir; PS = *Ph*PPS, *e*PPS, *Pr*PPS; abbreviations and structures summarised in Fig. 5) by direct reaction of $[RhF(CO)(PPh_3)_2]$ with PSH in toluene, $Et_3N$ being added for M = Ir. We also describe oxidative addition reactions with a range of electrophiles with the objective of establishing if electrophilic attack occurred at sulfur or the metal and if replacement of chloride by thiolate in $[RhCl(CO)P_2]$ (P = tertiary phosphine) type complexes modified the chemistry.

The comparative lability of the fluoride ligand in the complexes $[MF(CO)(PPh_3)_2]$ permits high yield syntheses of the complexes $[M(PS)(CO)(PPh_3)_2]$ by direct reaction with one equivalent of the thiol. In our hands reaction of the chloro-complexes with lithium or sodium salts of the phosphinothiol gave mixtures and significantly lower yields of the required product. The complexes **9** to **14** were isolated as moderately air-stable yellow solids and analytical and spectroscopic data are summarised in Table 4.

The IR spectra show strong absorptions in the range 1947–1976 $cm^{-1}$ assigned to $\nu$(CO). It is at first sight somewhat surprising that the CO stretching frequency is higher for the complexes with PS ligands with ethylene or trimethylene backbones than for those with a phenyl group linking P and S (*Ph*PPS). This may be due to the saturated hydrogen backbones conferring more flexibility on the ligand. A similar effect is observed for [Ir(*Pr*PPS)(CO)($PPh_3$)] **14** and [Ir(*Ph*PPS)(CO)-($PPh_3$)] **13**, where $\nu$(CO) is 50 $cm^{-1}$ higher for the complex with the trimethylene bridge. The $^1H$ and $^{31}P$ NMR spectra were in accord with a square planar geometry of the complexes with *trans* phosphorus donors, as shown by X-ray crystallography.[6]

### Syntheses of complexes of the type $[IrH(PS)_2(CO)]$ (PS = *Ph*PPS 15 or *Pr*PPS) 16

Reaction of $[IrF(CO)(PPh_3)_2]$ with 2 equivalents of *Ph*PPSH or *e*PPSH in the presence of diethylamine as base gave the complexes $[IrH(PhPPS)_2(CO)]$ **15** or $[IrH(PrPPS)_2(CO)]$ **16** in good yield as pale yellow powders. Complex **15** was identical to that prepared earlier from $[IrCl(CO)(PPh_3)_2]$, and **16** is directly analogous. Analytical and spectroscopic data for (Table 4) **16** are consistent with its formulation as an octahedral iridium(III) complex.

### Reactions of [Rh(*Ph*PPS)(CO)($PPh_3$)] 9

Reactions of complex **9** with a range of electrophiles have been investigated, and these are summarised in Scheme 2. The reaction with HCl gave a complex, intractable mixture of products that could not be separated. However with excess of $HBF_4{\cdot}OEt_2$ in dry $CH_2Cl_2$ at room temperature a near quantitative yield was obtained of the deep purple dimeric cation $[Rh_2H_2(PhPPS)_2(CO)_2(PPh_3)_2]^{2+}$ **17** isolated as the $[BF_4]^-$ salt. The complex is moderately stable in air both as a solid and in

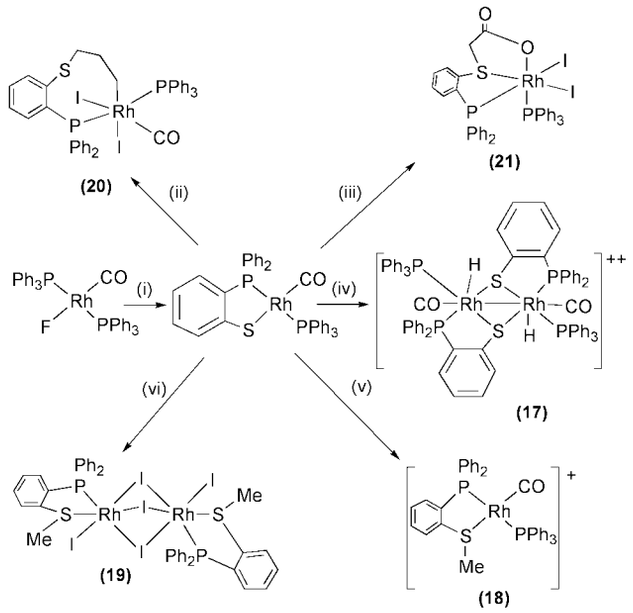


**Scheme 2** Summary of the synthesis and reactions of $[Rh(Ph_2PC_6H_4$-S-2)(CO)($PPh_3$)$_2$] **9**. (i) ArSH in toluene. (ii) $I(CH_2)_3I$ in $CH_2Cl_2$. (iii) Excess of $ICH_2CO_2H$ in benzene. (iv) $HBF_4{\cdot}Et_2O$ in $CH_2Cl_2$. (v) [MeO][$BF_4$] in $CH_2Cl_2$. (vi) Excess of MeI in benzene. All reactions at room temperature.

solution. The IR spectrum shows a single intense band at 2050 $cm^{-1}$ assigned to $\nu$(CO) and a broad bond at around 1090 $cm^{-1}$ due to the $[BF_4]^-$ counter ion. The FAB mass spectrum displays a peak at $m/z = 687$ due to $[M]^{2+}$ and also peaks at $m/z = 1082$ ($[M - H - CO - PPh_3]^+$) and 658 ($[M - 2CO]^{2+}$). Reaction of **17** with $Et_3N$ in methanol results in the quantitative regeneration of complex **9**, confirming an unusual example of reversible, pH-dependent formation of a thiolate-bridged metal–metal bond. However despite the clear evidence for the presence of protons from the reaction with base, we were unable to detect any $^1H$ NMR resonances attributable to metal hydride in the range $\delta$ +10 to −30. This may be due to a rapid hydrogen exchange process between the metal and sulfur sites, but the hydride resonances still could not be detected at lower temperatures. It is also possible that they are obscured by other intense peaks in the spectrum. The $^{31}P$ NMR revealed a complex second order spectrum which was consistent with the solid state structure discussed below.

The formation of the dimeric cation **17** presumably occurs *via* initial protonation at the metal to give $[RhH(FBF_3)$-(*Ph*PPS)(CO)($PPh_3$)] followed by displacement of the weakly bond $[BF_4]^-$ anion by the thiolate sulfur of an adjacent molecule. A precedent is found in the complex $[IrH(FBF_3)$-$Cl(CO)(PPh_3)_2]$ where a crystal structure confirmed the presence of an F-bound $[BF_4]^-$ anion.[25] Further support for the possibility of bridging hydrides in **17** comes from protonation of the complex $[Ir_2H_2(SBu^t)_2(CO)_2(PPh_3)_2]$ that gave $[Ir_2H_2$-$(\mu$-H)$(SBu^t)_2(CO)_2(PPh_3)_2]^+$ in which there is a single hydride bridging between the two iridiums.[26]

**The crystal stucture of $[Rh_2H_2(phPPS)_2(CO)_2(PPh_3)_2]^{2+}$ 17.** A ZORTEP representation of the molecular structure of complex **17** is shown in Fig. 6 and selected bond lengths and angles are displayed in Table 5. The geometry about each Rh is distorted octahedral (including the Rh–Rh bond) with each Rh atom lying above the P,P,S,S plane. There are vacant sites approximately *trans* to P(2) and P(4) which could accommodate the hydride ligands. The molecule is folded about the S–S vector to give a butterfly type structure, and the Rh–Rh distance is typical for a metal–metal single bond. The Rh–S distances for the bridging thiolates are significantly different [Rh(1)–S(1) 2.309(2), Rh(2)–S(1) 2.376(2), Rh(1)–S(2) 2.412(2), Rh(2)–S(2)

**Table 4** Phosphinothiolate complexes of rhodium(I) and iridium(I)

| Complex | Colour | Elemental analysis (%)[a] C | H | $\nu$(CO)[b] | NMR ($\delta$, $J$/Hz)[c] $^{31}$P | $^{1}$H | MS[d] ($m/z$) |
|---|---|---|---|---|---|---|---|
| **9** [Rh(*Ph*PPS)(CO)($PPh_3$)] | Pale yellow | 64.9 (64.7) | 4.1 (4.3) | 1962 | 63.5 (dd), 33.4 (dd), $J_{Rh-P}$ = 130.4, $J_{P-P}$ = 301.1 | 6.8–7.8 (m) (29 H, phenyl group) | 687 ($M^+$) |
| **10** [Rh(*Pr*PPS)(CO)($PPh_3$)] | Yellow orange | 60.1 (60.2) | 5.4 (5.4) | 1952 | 87.5 (dd), 32.8 (dd), $J_{Rh-P}$ = 127.3, $J_{P-P}$ = 287.6 | 6.8–7.8 (m) (19 H, aromatic), 2.5–2.7 (br) (2 H, CH), 1.37 (d), 1.31 (d), 1.20 (d), 1.14 (d) (12 H, $CH_3$) | 653 ($M^+$) |
| **11** [Rh(*e*PPS)(CO)($PPh_3$)] | Yellow | 62.1 (62.1) | 4.5 (4.6) | 1976 | | 6.8–8.4 (m) (25 H, aromatic), 2.2–3.7 (br) (4 H, $CH_2$) | 639 ($M^+$) |
| **12** [Rh(*e**PPS)(CO)($PPh_3$)] | Yellow | 62.5 (62.5) | 5.0 (4.9) | 1951 | 68.2 (dd), 59.9 (dd), $J_{Rh-P}$ = 133.4, $J_{P-P}$ = 304.2 | 7.0–8.0 (m) (25 H, aromatic), 2.9–3.2 (m) (2 H, $CH_2$), 2.4–2.7 (m) (1 H, CH), 1.3–1.5 (d) (3 H, $CH_3$) | 653 ($M^+$) |
| **13** [Ir(*Ph*PPS)(CO)($PPh_3$)] | Yellow | 57.2 (57.3) | 3.8 (3.8) | 1947 | 55.0 (d), 25.9 (d), $J_{P-P}$ = 303.1 | 6.7–6.9 (m) (29 H, aromatic) | 776 ($M^+$) |
| **14** [Ir(*Pr*PPS)(CO)($PPh_3$)] | Yellow | 52.5 (52.6) | 4.6 (4.7) | 1997 | 53.1 (d), 6.84 (d), $J_{P-P}$ = 380.0 | 6.7–7.9 (m) (19 H, aromatic), 2.3–3.0 (br) (2 H, CH), 0.8–1.5 (m) (12 H, $CH_3$) | 708 ($M^+$) |
| **15** [IR(H)(*Ph*PPS)$_2$(CO)] | Yellow | 55.1 (55.0) | 3.6 (3.6) | 2026, $\nu$(Ir–H) 2098w | 37.08 (d), 23.84 (d), $^2J_{P-P}$ = 307.2 | 6.7–8.0 (m) (28 H, aromatic), −11.29 (dd) (1 H, hydride), $^2J_{H-P}$ = 8.85 | 778 $(M - CO - H)^+$ |
| **16** [Ir(H)(*Pr*PPS)$_2$(CO)] | Yellow | 50.3 (50.3) | 4.5 (4.5) | 2018, $\nu$(Ir–H) 2112w | −28.3(s) | 7.2–8.2 (m) (20 H, aromatic), 2.0–3.9 (m) (12 H, $CH_2$), −11.6 (d) (1 H, hydride, $J_{P-H}$ = 11.2) | 740 ($M^+$) |
| **17** [$Rh_2$(*Ph*PPS)$_2$(CO)$_2$($PPh_3$)$_2$][$BF_4$]$_2$ | Purple | 56.2 (56.8) | 3.9 (3.9) | 2050 | 62.0 (d), 15.5 (d) | 6.4–8.0 (m) (aromatic) | 1082 $(M - CO - PPh_3 - H)^+$ |
| **18** [Rh(*Ph*PPSMe)(CO)($PPh_3$)][$BF_4$] | Purple | 57.9 (57.9) | 4.1 (4.1) | 2014 | 61.8 (dd), $^1J_{P-Rh}$ = 115.2, 27.5 (dd), $^1J_{P-Rh}$ = 123.3, $^2J_{P-P}$ = 272.9 | 6.5–8.0 (m) (29 H, aromatic), 1.8 (s) (3 H, $SCH_3$) | 701 ($M^+$) |
| **19** [$Rh_2$(μ-I)$_2$(I)$_4$(*Ph*PPSMe)$_2$] | Deep red | 29.0 (28.8) | 2.2 (2.2) | | 70.5 (dd), $^1J_{P-Rh}$ = 115.2 | 6.7–8.2 (m) (20 H, aromatic), 1.8 (s) (3 H, $CH_3$) | 701 ($M^+$) |
| **20** [$RhI_2$(*Ph*PPS($CH_2$)$_3$)(CO)($PPh_3$)] | Bright red | 54.1 (54.3) | 3.7 (3.6) | 2062 | 61.2 (dd), $^1J_{P-Rh}$ = 136.4, 25.8 (dd), $^1J_{P-Rh}$ = 121.2, $^2J_{P-P}$ = 16.2 | 6.7–8.1 (m) (29 H, aromatic), 0.7–2.4 (m, br) (6 H, $CH_2$) | 730 $(M - 2I)^+$ |
| **21** [$RhI_2$(*Ph*PPS$CH_2CO_2$)($PPh_3$)] | Deep red | 46.9 (47.0) | 3.3 (3.3) | 1652 | 48.2 (dd), 4.9 (dd), $^2J_{P-P}$ = 545.7 | 6.8–7.5 (m) (29 H, aromatic), 2.75 (d) (1 H, $CH_2$), 2.20 (d) (1 H, $CH_2$), $^2J_{H-H}$ = 17.3 | 971 ($M^+$) |
| **22** *trans*-[$RhI_3$(CO)($PPh_3$)$_2$] | Deep orange | 43.0 (42.9) | 2.9 (2.9) | 2082 | 48.2 (d), $^1J_{P-Rh}$ = 76.8 | 6.8–8.5 (m) (aromatic) | 881 $(M - CO - I)^+$ |

[a] Calculated values in parentheses. [b] As Nujol mulls, in $cm^{-1}$. [c] In $CDCl_3$ solution. [d] FAB mass spectra in 3-nitrobenzyl alcohol matrix.

**Table 5** Selected bond lengths (Å) and angles (°) for compound **17**

| | | | |
|---|---|---|---|
| Rh(1)–C(1) | 1.933(9) | P(1)–C(21) | 1.828(8) |
| Rh(1)–S(1) | 2.309(2) | P(1)–C(31) | 1.840(8) |
| Rh(1)–P(1) | 2.320(2) | P(2)–C(81) | 1.833(9) |
| Rh(1)–P(2) | 2.395(2) | P(2)–C(61) | 1.833(8) |
| Rh(1)–S(2) | 2.412(2) | P(2)–C(71) | 1.836(8) |
| Rh(1)–Rh(2) | 2.746(2) | S(2)–C(42) | 1.784(8) |
| Rh(2)–C(2) | 1.886(9) | P(3)–C(41) | 1.815(8) |
| Rh(2)–P(3) | 2.320(2) | P(3)–C(51) | 1.816(8) |
| Rh(2)–S(2) | 2.321(2) | P(3)–C(91) | 1.829(8) |
| Rh(2)–S(1) | 2.376(2) | P(4)–C(111) | 1.814(8) |
| Rh(2)–P(4) | 2.440(2) | P(4)–C(101) | 1.830(8) |
| S(1)–C(12) | 1.777(8) | C(1)–O(1) | 1.090(10) |
| P(1)–C(11) | 1.816(8) | C(2)–O(2) | 1.136(11) |
| | | | |
| C(1)–Rh(1)–S(1) | 161.7(2) | C(2)–Rh(2)–P(3) | 91.0(3) |
| C(1)–Rh(1)–P(1) | 96.5(2) | C(2)–Rh(2)–S(2) | 161.9(3) |
| S(1)–Rh(1)–P(1) | 86.75(7) | P(3)–Rh(2)–S(2) | 87.02(8) |
| C(1)–Rh(1)–P(2) | 99.2(2) | C(2)–Rh(2)–S(1) | 97.2(3) |
| S(1)–Rh(1)–P(2) | 98.08(7) | P(3)–Rh(2)–S(1) | 158.88(7) |
| P(1)–Rh(1)–P(2) | 98.70(8) | S(2)–Rh(2)–S(1) | 79.16(8) |
| C(1)–Rh(1)–S(2) | 92.9(2) | C(2)–Rh(2)–P(4) | 98.3(3) |
| S(1)–Rh(1)–S(2) | 78.68(7) | P(3)–Rh(2)–P(4) | 105.13(8) |
| P(1)–Rh(1)–S(2) | 159.14(7) | S(2)–Rh(2)–P(4) | 99.54(7) |
| P(2)–Rh(2)–S(2) | 98.07(8) | S(1)–Rh(2)–P(4) | 92.96(8) |
| C(1)–Rh(1)–Rh(2) | 106.7(2) | C(2)–Rh(2)–Rh(1) | 107.6(3) |
| S(1)–Rh(1)–Rh(2) | 55.27(5) | P(3)–Rh(2)–Rh(1) | 105.98(6) |
| P(1)–Rh(1)–Rh(2) | 106.32(6) | S(2)–Rh(2)–Rh(1) | 56.09(5) |
| P(2)–Rh(1)–Rh(2) | 141.18(6) | S(1)–Rh(2)–Rh(1) | 52.97(6) |
| S(2)–Rh(1)–Rh(2) | 52.99(5) | P(4)–Rh(2)–Rh(1) | 138.71(6) |

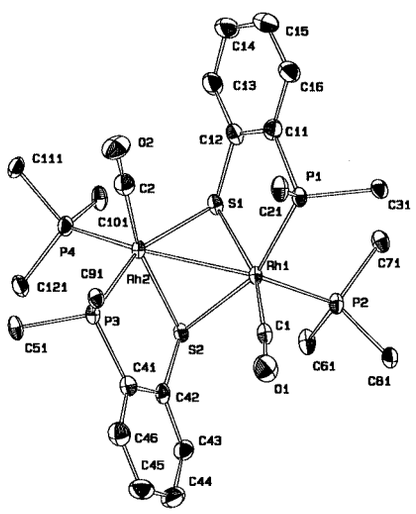


**Fig. 6** A ZORTEP representation of the structure of $[Rh_2H_2(\mu\text{-}Ph_2PC_6H_4S\text{-}2)_2(CO)_2(PPh_3)_2]^{2+}$ **17** showing the atom labelling scheme. The tertiary phosphine phenyl groups are omitted for clarity.

2.321(2) Å] probably as a consequence of the presence of the chelated P,S ring system.

**With $[Me_3O][BF_4]$ or MeI.** Reaction of complex **9** with $[Me_3O][BF_4]$ in dry $CH_2Cl_2$ gave the purple rhodium(I) cation $[Rh(PhPPSMe)(CO)(PPh_3)]^+$ **18** in high yield, isolated as the $[BF_4]^-$ salt. The IR spectrum showed an intense band due to $\nu$(CO) at 2014 $cm^{-1}$ (see Table 4). This is 36 $cm^{-1}$ lower than the value for complex **17**, consistent with alkylation taking place at sulfur rather than the metal and retention of the rhodium(I) oxidation state.

The oxidative addition of MeI is a crucial step in the carbonylation of methanol in the Monsanto process, and we have investigated the reaction of complex **9** with an excess of methyl iodide. In benzene at room temperature the deep red dimeric complex $[Rh_2I_6(PhPPSMe)_2]$ **19** is formed in high yield. GC analysis of the reaction mixture indicated that acetone had been formed in virtually quantitative yield, presumably *via* methylation of an acetyl intermediate. The formation of acetone is not

**Table 6** Selected bond lengths (Å) and angles (°) for compound **19**

| | | | |
|---|---|---|---|
| Rh–P | 2.272(3) | I(1)–Rh#1 | 2.7602(14) |
| Rh–S | 2.355(4) | S–C(12) | 1.801(12) |
| Rh–I(2) | 2.659(2) | S–C | 1.831(14) |
| Rh–I(3) | 2.6603(14) | P–C(11) | 1.808(13) |
| Rh–I(1) | 2.683(2) | P–C(31) | 1.807(13) |
| Rh–I(1)#1 | 2.7602(14) | P–C(21) | 1.828(14) |
| | | | |
| P–Rh–S | 86.10(12) | P–Rh–I(1)#1 | 176.02(10) |
| P–Rh–I(2) | 91.93(10) | S–Rh–I(1)#1 | 90.09(9) |
| S–Rh–I(2) | 84.12(10) | I(2)–Rh–I(1)#1 | 86.53(4) |
| P–Rh–I(3) | 89.75(10) | I(3)–Rh–I(1)#1 | 93.97(4) |
| S–Rh–I(3) | 174.11(10) | I(1)–Rh–I(1)#1 | 81.62(4) |
| I(2)–Rh–I(3) | 91.85(5) | Rh–I(1)–Rh#1 | 98.38(4) |
| P–Rh–I(1) | 99.88(9) | C(12)–S–C | 96.5(6) |
| S–Rh–I(1) | 95.65(10) | C(12)–S–Rh | 103.4(5) |
| I(2)–Rh–I(1) | 168.16(5) | C–S–Rh | 114.0(5) |
| I(3)–Rh–I(1) | 89.17(4) | | |

Symmetry relation: #1 $-x, -y, -z$.

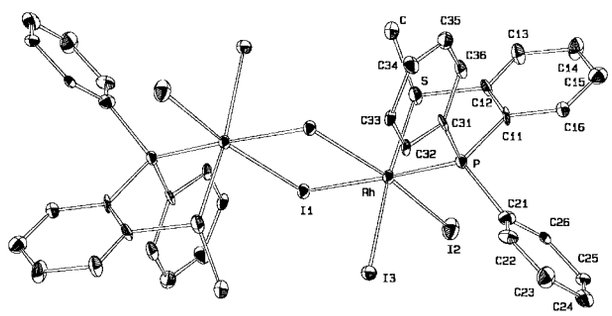


**Fig. 7** A ZORTEP representation of the structure of $[Rh_2I_6(Ph_2PC_6H_4SMe\text{-}2)_2]$ **19**, showing the atom labelling scheme.

unexpected for these systems, and is observed as a by-product in the carbonylation of methanol.[27] The availability of sulfur as an additional site for alkylation has a significant effect on the course of the reaction, and little or no acetone is formed when $[RhCl(CO)(PPh_3)_2]$ is treated with an excess of MeI under similar conditions.

**Crystal structure of $[Rh_2I_6(PhPPSMe)_2]$ 19.** The X-ray crystal structure is shown in Fig. 7 and selected bond lengths and angles appear in Table 6. The geometry about each rhodium(III) atom of the dimer is approximately octahedral with a double iodide bridge. The bond distances and angles for the $Rh_2I_6$ unit are similar to those reported for $[Rh_2(MeCO)_2I_6(CO)_2]^{2-}$.[28] The phosphinothiolate ligand has been alkylated at sulfur to give the corresponding bidentate thioether and the Rh–P and Rh–S distances are very similar to those found in $[Rh(ePPSMe)_2]BF_4$.[29]

**With 1,3-diiodopropane.** Reaction of complex **9** with an excess of $I(CH_2)_3I$ in dry dichloromethane for 24 h at room temperature gave **20** as a bright orange powder in *ca.* 55% yield. The elemental analysis suggested the stochiometry 'Rh(*Ph*PSS)$(CH_2)_3I_2$(CO)$(PPh_3)$' consistent with oxidative addition of the diiodopropane unit. The IR showed a single strong band at 2062 $cm^{-1}$, the increase from that found in **9** being consistent with oxidative addition at the metal. The $^{31}P$ NMR showed two doublets of doublets at $\delta$ 61.2 and 25.8 consistent with two inequivalent phosphine ligands. The FAB mass spectrum shows a strong peak at $m/z = 658$ corresponding to $[M - (CH_2)_3 - 2I - CO]^+$ with appropriate isotope distribution.

The first step of the reaction is presumably oxidative addition of one end of the diiodopropane to the $Rh^I$ or at S to give $[RhI(CH_2CH_2CH_2I)(PhPPS)(CO)(PPh_3)_2]$ or $[Rh(PhPPSCH_2CH_2CH_2I)(CO)(PPh_3)]^+I^-$. These possibilities cannot be distinguished, but the fact that no CO insertion product is

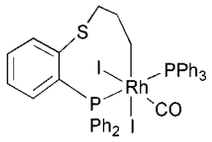


**Fig. 8** Proposed structure for $[RhI_2(Ph_2PC_6H_4S(CH_2)_3)(CO)(PPh_3]$ **20**.

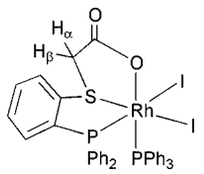


**Fig. 9** Proposed structure for $[RhI_2(Ph_2PC_6H_4SCH_2CO_2)(PPh_3)]$ **21**.

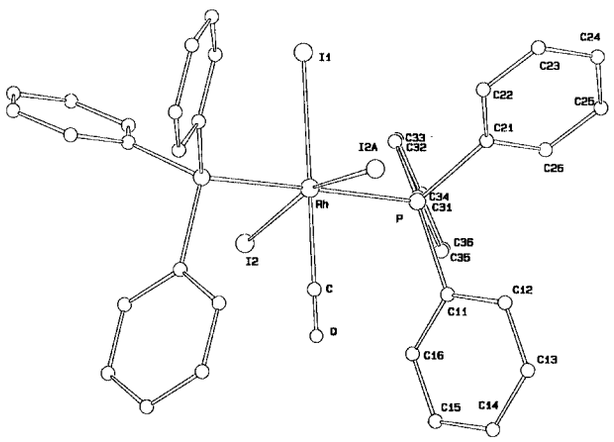


**Fig. 10** A ZORTEP representation of the structure of $[RhI_3(CO)(PPh_3)_2]$ **22**, showing the atom labelling scheme.

observed, and the nature of the product **19** of the reaction with $Me_3O^+BF_4^-$, suggest initial attack may be at sulfur. Oxidative addition of the second $CH_2I$ group and co-ordination of the iodide counter ion gives the final product **20**, for which we propose the structure shown in Fig. 8. The formation of the chelated alkyl derivative presumably prevents insertion of CO to give a co-ordinated acetyl group.

**With iodoacetic acid.** An excess of iodoacetic acid reacted with complex **9** in benzene at room temperature to give **21** as a deep red powder in about 50% isolated yield. The complex is stable in air both in the solid state and in solution, the elemental analysis being consistent with the stoichiometry '$RhI_2$(*Ph*PPS)-$(CH_2CO_2)(PPh_3)$'. The IR spectrum shows a strong band at 1652 $cm^{-1}$ assigned to a carboxyl group, but no band attributable to a terminally bond carbonyl ligand. $^1H$ NMR showed the expected multiplet for the aromatic protons and a pair of doublets at $\delta$ 2.20 and 2.75 assigned to the methylene protons and suggests metal binding by the carboxylate oxygen. The $^{31}P$ NMR comprised two doublets of doublets at $\delta$ 48.2 and 4.9 consistent with two inequivalent phosphine ligands bound to Rh. An intense peak in the MS at $m/z = 971$ corresponds to $[M]^+$ and a weaker peak at $m/z = 844$ to $[M - I]^+$. Based on the analytical and spectroscopic data we assign the structure shown in Fig. 9. The loss of the CO ligand suggests a multiple series of insertion/addition reactions, as with methyl iodide, but we were unable to identify the eventual fate of the CO in this case.

A by-product of the reaction, isolated by recrystallisation as a red solid in *ca.* 15% yield, is $[RhI_3(CO)(PPh_3)_2]$ **22**. Crystals suitable for structure determination were grown from dichloromethane–methanol.[30] A ZORTEP representation of the structure appears in Fig. 10. The geometry about the Rh is pseudo octahedral with the two phosphorus donors in *trans* locations. Such trihalogenorhodium(III) complexes have been observed before[31] but isolated in very low yield and identified by NMR spectroscopy. The Rh–P distances are closely similar to those in $[Rh(CH_3)I_2(PPh_3)_2]$[32] and the Rh–I distances are close to those found in $[Rh(COCH_3)I_2(Ph_2PCH_2CH_2PPh_2)]$.[33]

## Conclusion

We have shown that reaction of a fluoro precursor with bulky aromatic thiolates provides a convenient high yield route to complexes of the types $[M(SAr)(CO)(PPh_3)_2]$ (M = Ir) and $[M_2(\mu\text{-}SAr)_2(CO)_2(PPh_3)_2]$ (M = Rh). These have been shown to be effective hydroformylation catalysts. The monomeric phosphinothiolate complex [Rh(*Ph*PPS)(CO)($PPh_3$)] can be prepared analogously and its reactions clearly show that, with the exception of the proton, electrophilic attack takes place at the thiolate sulfur. This causes such reactions to take a quite different course from that for complexes where thiolate is replaced by halide or the thiolate is bridging and much less susceptible to electrophilic attack. By contrast, protonation with acids with weakly co-ordinating anions occurs at the metal with an unusual example of reversible thiolate bridge formation.

## Experimental

Unless stated otherwise, all reactions were carried out under an atmosphere of dinitrogen using conventional Schlenk glassware and solvents were dried using established procedures and distilled under dinitrogen immediately prior to use. IR spectra were recorded on a Perkin-Elmer Paragon FT-IR spectrometer as Nujol mulls and $^1H$ and $^{31}P$ NMR spectra on a JEOL EX270 spectrometer in $CDCl_3$ solution. Elemental analyses were determined on a Perkin-Elmer 240 instrument at the University of Essex. The complexes $[MF(CO)(PPh_3)_2]$ (M = Rh or Ir) were made by the literature method.[34] The thiols, TIPBTH,[35] DMBTH[35] and TPSBTH[36] and phosphinothiols *Ph*PPSH, *e*PPSH,[37] *e**PPSH[37] and *Pr*PPSH[37] were also prepared by published routes.

### Preparations

***trans*-[Rh(DCBT)(CO)($PPh_3$)$_2$] 1.** *trans*-[RhF(CO)($PPh_3$)$_2$] (0.10 g, 0.15 mmol) and the thiol DCBTH (0.027 g, 15 mmol) were stirred at room temperature in toluene (30 ml) for 45 min to give an orange solution. The solvent was removed under reduced pressure and the residue crystallised from $CH_2Cl_2$–MeOH as a yellow-orange microcrystalline powder in 85% yield.

***trans*-[Rh(TPSBT)(CO)($PPh_3$)$_2$] 2.** This compound was prepared in a similar manner to **1** from *trans*-[RhF(CO)($PPh_3$)$_2$] (0.1 g, 0.15 mmol) and the thiol TPSBTH (0.055 g, 0.15 mmol). Yield 70%.

**[$Rh_2$(μ-DMBT)$_2$(CO)$_2$($PPh_3$)$_2$] 3.** This compound was prepared in a similar manner to **1** from *trans*-[RhF(CO)($PPh_3$)$_2$] (0.1 g, 0.15 mmol) and the thiol DMBTH (0.020 g, 0.15 mmol). Yield 80%.

**[$Rh_2$(μ-TIPBT)$_2$(CO)$_2$($PPh_3$)$_2$] 4.** This compound was prepared in a similar manner to compound **1** from *trans*-[RhF(CO)($PPh_3$)$_2$] (0.1 g, 0.15 mmol) and the thiol TIPBTH (0.035 g, 0.15 mmol). Yield 83%.

***trans*-[Ir(DCBT)(CO)($PPh_3$)$_2$] 5.** To a solution of *trans*-[IrF(CO)($PPh_3$)$_2$] (0.1 g, 0.13 mmol) in toluene (25 $cm^3$) was added 1 equivalent of the thiol DCBTH (0.023 g, 0.13 mmol). The solution was stirred at room temperature for 45 min. The volume was reduced under vacuum and the residue recrystallised from $CH_2Cl_2$–MeOH. Yield 95%.

***trans*-[Ir(TPSBT)(CO)($PPh_3$)$_2$] 6.** This compound was prepared in a similar manner to **5** from *trans*-[IrF(CO)($PPh_3$)$_2$] (0.1 g, 0.13 mmol) and the thiol TPSBTH (0.048 g, 0.13 mmol). Yield 90%.

***trans*-[Ir(DMBT)(CO)($PPh_3$)$_2$] 7.** This compound was prepared in a similar manner to **5** from *trans*-[IrF(CO)($PPh_3$)$_2$] (0.1 g, 0.13 mmol) and the thiol DMBTH (0.018 g, 0.13 mmol). Yield 40%.

***trans*-[Ir(TIPBT)(CO)($PPh_3$)$_2$] 8.** To a solution of *trans*-[IrF(CO)($PPh_3$)$_2$] (0.1 g, 0.13 mmol), TIPBTH (0.031 g, 0.13 mmol) was added. After stirring in toluene (25 ml) for 1 hour a green solution was obtained. Reduction of the solvent under vacuum yielded a green oily product. The crude material was then redissolved in the minimum amount of $CH_2Cl_2$ and chromatographed on a column using silica gel as the stationary phase (Kieselgel 60, Fluka) and eluted with $CH_2Cl_2$. The green solution was collected and impurities remained at the top of the column. Yield 43% as a yellow solid.

**[Rh(*Ph*PPS)(CO)($PPh_3$)] 9.** To a solution of *trans*-[RhF(CO)($PPh_3$)$_2$] (0.1 g, 0.15 mmol) in toluene (25 $cm^3$) was added 1 equivalent of the phosphinothiol *Ph*PPSH (0.044 g, 0.15 mmol). The solution was stirred for 45 min, the volume reduced under reduced pressure and the residue recrystallised as a pale yellow solid from $CH_2Cl_2$–MeOH. Yield 95%.

**[Rh(*Pr*PPS)(CO)($PPh_3$)] 10.** This compound was prepared in a similar manner to **9** from *trans*-[RhF(CO)($PPh_3$)$_2$] (0.1 g, 0.15 mmol) and the phosphinothiol *Pr*PPSH (0.039 g, 0.15 mmol), yield 90%.

**[Rh(*e*PPS)(CO)($PPh_3$)] 11.** This compound was prepared in a similar manner to **9** from *trans*-[RhF(CO)($PPh_3$)$_2$] (0.1 g, 0.15 mmol) and the phosphinothiol *e*PPSH (0.037 g, 0.15 mmol), yield 80%.

**[Rh(*e**PPS)(CO)($PPh_3$)] 12.** This compound was prepared in a similar manner to **9** from *trans*-[RhF(CO)($PPh_3$)$_2$] (0.1 g, 0.15 mmol) and the phosphinothiol *e**PPSH (0.039 g, 0.15 mmol), yield 87%.

**[Ir(*Ph*PPS)(CO)($PPh_3$)] 13.** To a solution of *trans*-[IrF(CO)($PPh_3$)$_2$] (0.1 g, 0.13 mmol) in toluene (25 $cm^3$) was added 1 equivalent of the phosphinothiol *Ph*PPSH (0.039 g, 0.13 mmol). The solution was stirred for 45 min in the presence of $NEt_3$, the volume reduced under reduced pressure and the residue recrystallised as a pale yellow solid from $CH_2Cl_2$–MeOH. Yield 72%.

**[Ir(*Pr*PPS)(CO)($PPh_3$)] 14.** This compound was prepared in a similar manner to **13** from *trans*-[IrF(CO)($PPh_3$)$_2$] (0.1 g, 0.13 mmol) and the phosphinothiol *Pr*PPSH (0.034 g, 0.13 mmol), yield 90%.

**[Ir(H)(*Ph*PPS)$_2$(CO)] 15.** This compound was prepared in a similar manner to **13** from *trans*-[IrF(CO)($PPh_3$)$_2$] (0.1 g, 0.13 mmol) and the phosphinothiol *Ph*PPSH (0.039 g, 0.13 mmol), but no $NEt_3$ was added, yield 87%.

**[Ir(H)(*Pr*PPS)$_2$(CO)] 16.** This compound was prepared in a similar manner to **15** from *trans*-[IrF(CO)($PPh_3$)$_2$] (0.1 g, 0.13 mmol) and the phosphinothiol *Pr*PPSH (0.034 g, 0.13 mmol), yield 87%.

**[Rh$_2$(*Ph*PPS)$_2$(CO)$_2$($PPh_3$)$_2$][$BF_4$]$_2$ 17.** To a $CH_2Cl_2$ solution (20 $cm^3$) of complex **9** (0.1 g, 0.146 mmol) was added an excess of $HBF_4$ (0.03 mg, 0.35 mmol); an immediate change from a bright yellow to a dark purple was observed. The mixture was stirred for 1 hour and then the solvent removed under vacuum. The residue was redissolved in the minimum amount of $CH_2Cl_2$ and precipitated with *n*-pentane as a fine, dark red-purple powder **17**, yield 80%.

**[Rh(*Ph*PPSMe)(CO)($PPh_3$)][$BF_4$] 18.** To a benzene solution (25 ml) of complex **9** (0.1 g, 0.146 mmol) was added an excess of [$Me_3O$][$BF_4$] (0.05 g, 0.350 mmol). After stirring for 30 min a precipitate started to form and a change from a bright yellow to a dark purple was observed. The mixture was stirred for one hour and then the deep purple precipitate filtered off, redissolved in the minimum amount of $CH_2Cl_2$ and precipitated with *n*-pentane as a fine, deep purple powder **18**, yield 65%.

**[Rh$_2$(μ-I)$_2$(I)$_4$(*Ph*PPSMe)$_2$] 19.** To a solution of complex **9** (0.1 g, 0.146 mmol) in benzene (10 $cm^3$), was added MeI (0.8 $cm^3$) and the mixture allowed to stir for 24 hours. During this time a change from bright yellow to deep red was observed. The solvent was removed under vacuum to give a reddish black residue, which was redissolved in the minimum of $CH_2Cl_2$ and layered with MeOH. On standing for 24 hours a deep red microcrystalline product **19** was isolated. Yield 52%.

**[RhI$_2$(*Ph*PPS(CH$_2$)$_3$)(CO)($PPh_3$)] 20.** To a $CH_2Cl_2$ solution (25 ml) of complex **9** (0.1 g, 0.146 mmol) was added 1,3-diiodopropane (0.8 $cm^3$) and the mixture stirred for 24 hours. The solvent was then removed *in vacuo* and the orange residue redissolved in the minimum amount of $CH_2Cl_2$ and precipitated with *n*-pentane yielding the compound **20** as a bright orange powder. Yield 55%.

**[RhI$_2$(*Ph*PPSCH$_2$CO$_2$)($PPh_3$)] 21.** This compound was synthesized analogously to **20** using an excess of iodoacetic acid, yield 52%.

***trans*-[RhI$_3$(CO)($PPh_3$)$_2$] 22.** This compound was obtained from the previous reaction as a by-product. Purification was achieved by recrystallisation from $CH_2Cl_2$–MeOH, final yield 15%.

### Catalysis experiments

Hydroformylation experiments were carried out at the Instituto de Catalisis y Petroleoquimica, Consejo Superior de Investigaciones Cientificas, (C.S.I.C.), Madrid, Spain, in a 150 $cm^3$ stainless steel autoclave with a magnetic stirrer and a glass inlet. The temperature was kept constant at 70 °C by using a double jacket water system circulate. Syngas ($H_2$:CO = 1:1) was introduced at a constant pressure of 5 bar from a gas reservoir. The fall of pressure in the autoclave was monitored with a transducer connected to an electric recorder. A solution of the precursor containing the substrate was placed in the evacuated autoclave and then heated to the required temperature. When thermal equilibrium was reached Syngas was introduced at 5 bar, and stirring was initiated. After each run the solution was analysed by GLC with a Hewlett-Packard 5940A chromatograph equipped with a 6 m × 1/8 in column of OV-17 on Chromosorb WHP.

### X-Ray data collection

**For complexes 5 and 17.** Intensity data were collected on an Enraf-Nonius CAD4 diffractometer[38] with monochromated Mo-Kα radiation ($\lambda$ = 0.71073 Å). Cell constants were obtained from least squares refinement of the setting angles of 25 centred reflections in the range $1.87 < \theta < 24.97°$. The data were collected in the $\omega$–$2\theta$ scan mode and three standard reflections were measured every 2 hours of exposure. Three standard reflections were measured every 200 to check the crystal orientation. The data were corrected for Lorentz and polarisation factors and an absorption correction was applied using psi scans of nine reflections.

**For complexes 4 and 19.** Intensity data were collected at the EPSRC service, Cardiff on a Delft-Instrument FAST-TV area detector diffractometer with graphite-monochromated Mo-Kα

**Table 7** Summary of X-ray structural data for complexes **4**, **5**, **17** and **19**

| | **4** $[Rh_2(\mu\text{-TIPBT})_2(CO)_2(PPh_3)_2]$ | **5** *trans*-$[Ir(DCBT)(CO)(PPh_3)_2]$ | **17** $[RhH_2(PhPPS)_2(CO)_2(PPh_3)_2][BF_4]_2$ | **19** $[Rh_2(\mu\text{-I})_2(I)_4(PhPPSMe)_2]$ |
|---|---|---|---|---|
| Empirical formula | $C_{68}H_{76}O_2P_2Rh_2S_2$ | $C_{43}H_{33}Cl_2IrOP_2S$ | $C_{74}H_{60}B_2F_8O_2P_4Rh_2S_2$ | $C_{19}H_{17}I_3PRhS$ |
| $M$ | 1257.17 | 922.79 | 1548.66 | 791.97 |
| Crystal system | Monoclinic | Triclinic | Triclinic | Monoclinic |
| Space group | $P2_1/n$ | $P\bar{1}$ | $P\bar{1}$ | $P2_1/n$ |
| $a$/Å | 13.529(4) | 9.2039(10) | 11.931(2) | 12.503(2) |
| $b$/Å | 33.568(10) | 11.600(2) | 13.554(9) | 12.982(5) |
| $c$/Å | 14.134(5) | 19.014(3) | 22.814(4) | 14.481(3) |
| $\alpha$/° | | 99.934(10) | 97.70(3) | |
| $\beta$/° | 104.69(5) | 95.243(10) | 97.870(10) | 92.51(5) |
| $\gamma$/° | | 106.744(10) | 97.41(4) | |
| $V$/Å$^3$ | 6209(3) | 1893.3(5) | 3581(3) | 2348.2(11) |
| $Z$ | 4 | 2 | 2 | 4 |
| $\mu$(Mo-K$\alpha$)/mm$^{-1}$ | 0.693 | 3.840 | 0.674 | 4.829 |
| $T$/K | 293 | 293 | 293 | 293 |
| Reflections collected | 20978 | 7071 | 13194 | 6872 |
| Independent reflections ($R_{ins}$) | 8986(0.1085) | 6616(0.0121) | 12610(0.0701) | 3276(0.0757) |
| Reflections observed | 5682 | 6098 | 9358 | 1980 |
| $R1$, $wR2$ | 0.0637, 0.1356 | 0.0222, 0.0575 | 0.0685, 0.1951 | 0.430, 0.0925 |

radiation ($\lambda = 0.71069$ Å).[39] Cell constants were obtained from least squares refinement of the setting angles of 250 reflections having $\theta = 2.34$–$25.09°$.

**Structure analysis and refinement.** The structures were all solved *via* direct methods[40] and refined on $F_o^2$ by full-matrix least squares.[41] All non-hydrogen atoms were anisotropic. The hydrogen atoms were included in idealised positions with $U_{iso}$ free to refine. The weighting scheme gave satisfactory results. The structure diagrams were produced by ZORTEP.[14] Crystallographic data for all four compounds are presented in Table 7.

CCDC reference number 186/2095.

See http://www.rsc.org/suppdata/dt/b0/b005588n/ for crystallographic files in .cif format.

## Acknowledgements

We are grateful to CONACYT for financial support to D. M., and to Dr P. Terreros at the Instituto de Catalisis y Petroleoquimica, C. S. I. C. Campus UAM, Madrid, Spain, for the facilities to carry out the catalytic experiments.

## References

1 M. El Amene, A. Maisonnat, F. Dahan and R. Poilblanc, *Nouv. J. Chim.*, 1991, **12**, 661.
2 A. Maisonnat and R. Poilblanc, *C.R. Acad Sci.*, *Ser. 2*, 1984, **298,** 69.
3 M. Pinnillos, E. Teresa, L. A. Oro, F. J. Lahoz, F. Bonati, and M. Tiripicchio-Camellini, *J. Chem. Soc.*, *Dalton Trans*, 1996, 989.
4 J. R. Dilworth and N. Wheatley, *Coord. Chem. Rev.*, 2000, **199,** 89.
5 J. R. Dilworth, J. R. Miller, N. Wheatley, M. Baker and G. Sunley, *J. Chem. Soc.*, *Chem. Commun.*, 1995, 1579.
6 M. Baker, M. F. Giles, A. G. Orpen, M. J. Taylor and R. J. Watt, *J. Chem. Soc.*, *Chem. Commun.*, 1995, 197.
7 L. Dahlenburg, K. Herbst and M. Kuhlein, *Z. Anorg. Chem.*, 1997, **623**, 250.
8 D. W. Stephan, *Inorg. Chem.*, 1984, **23**, 2207.
9 J. R. Dilworth, D. W. Griffiths and Y. Zheng, *J. Chem. Soc.*, *Dalton Trans.*, 1999, 1877.
10 M. Pinnillos, A. Eduque, J. A. Lopez, F. J. Lahoz and L. A. Oro, *J. Chem. Soc.*, *Dalton Trans*, 1995, 1391.
11 M. L. Amene, A. Maisonatt, F. Dahan, R. Pince and R. Poilblanc, *Organometallics*, 1985, **4**, 773.
12 A. Maisonnat, J.-J. Bonnet and R. Poilblanc, *Inorg. Chem.*, 1980, **19**, 3168.
13 J. Devillers, J.-J. Bonnet, D. D. Montazon and R. Poilblanc, *Inorg. Chem.*, 1980, **19**, 154.
14 L. Zsolnai, ZORTEP, an ellipsoid representation program, University of Heidelberg, 1994.
15 R. A. Jones and S. T. Schwab, *J. Cryst. Struct. Res.*, 1986, **16**, 577.
16 J.-J. Bonnet, P. Kalck and R. Poilblanc, *Inorg. Chem.*, 1977, **16**, 1514.
17 J. J. Garcia, H. Torrens, H. Adams, N. A. Bailey and P. Maitlis, *J. Chem. Soc.*, *Chem. Commun.*, 1991, 74.
18 S. Sirol and P. Kalck, *Nouv. J. Chim.*, 1997, **21**, 1129; E. Fernandez, A. Ruiz, S. Castillon, C. Claver, J. F. Piniella, A. Alvarez-Larena and G. Germain, *J. Chem. Soc.*, *Dalton Trans.*, 1995, 2137.
19 N. Ruiz, A. Polo, S. Castillon and C. Claver, *J. Mol. Catal.* (*A*), 1997, **137**, 93.
20 T. Bang, J. Molinier and P. Kalck, *J. Organomet. Chem.*, 1993, **455**, 219.
21 M. Dieguez, C. Claver, A. M. Masdeu-Bolto, A. Ruiz, P. W. N. M. van Leuwen and G. C. Schoemaker, *Organometallics*, 1999, **18**, 2107.
22 F. Monteil, R. Queau, and P. Kalck, *J. Organomet. Chem.*, 1994, **480**, 177.
23 A. Orejon, C. Claver, L. A. Oro, A. Elduque and M. T. Pinillos, *J. Mol. Catal.* (*A*), 1998, **136**, 279.
24 C. Claver, S. Castillon, N. Ruiz, G. Delogu, D. Fabbri and S. Gladiali, *J. Chem. Soc.*, *Chem. Commun.*, 1994, 1833.
25 B. Olgemuller, H. Bauer and W. J. Beck, *J. Organomet. Chem.*, 1981, **213,** C57.
26 J.-J. Bonnet, A. Thorez, A. Maissonat, J. Galy and R. Poilblanc, *J. Am. Chem. Soc.*, 1979, **101**, 5940.
27 L. S. Hegedus, S. Lo and D. E. Bloss, *J. Am. Chem. Soc*, 1973, **95**, 3040; N. E. Schore, C. Ilenda and R. G. Bergman, *J. Am. Chem. Soc.*, 1976, **98**, 7436.
28 G. W. Adamson, J. J. Daly and D. Forster, *J. Organomet. Chem.*, 1974, **71**, C17.
29 D. G. Dick and D. W. Stephan, *Can. J. Chem.* 1986, **64**, 1870.
30 Crystal data: $a = 24.092(4)$, $b = 9.662(3)$, $c = 16.819(4)$ Å, $\beta = 115.08(4)°$, monoclinic, space group $C2/c$. Owing to the poor quality of the crystal, we were not able to collect enough data fully to refine the structure, however by constraining all carbon atoms on the phenyl group a reasonable structure was determined and refined which was consistent well with analytical data.
31 M. C. Baird, J. T. Mague, J. A. Osborn and G. Wilkinson, *J. Chem. Soc. A*, 1967, 1347; A. J. Deeming and B. L. Shaw, *J. Chem. Soc. A*, 1969, 597; C. Rosslyn, D. J. Cole-Hamilton, R. Whyman, J. C. Barnes and M. C. Simpson, *J. Chem. Soc.*, *Dalton Trans.*, 1994, 1963.
32 J. A. Evans, D. R. Russell, A. Bright and B. L. Shaw, *Chem. Commun.*, 1971, 841.
33 K. G. Malloy and J. L. Petersen, *Organometallics*, 1995, **14**, 2931.
34 J. R. Fitzgerald, N. Y. Sakhab, R. S. Strange and V. P. Narutis, *Inorg. Chem.*, 1973, **12**, 1081.
35 P. J. Blower, J. R. Dilworth, J. P. Hutchinson and J. Zubieta, *J. Chem. Soc.*, *Dalton Trans.*, 1985, 1533.
36 E. Bloch, V. Eswarakishnan, M. Gernon, G. Oferi-Okai, C. Saha, K. Tong and J. Zubieta, *J. Am. Chem. Soc.*, 1989, **111**, 658.
37 P. J. Blower, J. R. Dilworth, G. J. Leigh, B. D. Neaves, F. B. Normanton, J. P. Hutchinson and J. Zubieta, *J. Chem. Soc.*, *Dalton Trans.*, 1985, 2647.
38 *CAD4 Operations Manual*, Enraf-Nonius, Delft, 1977.
39 A. A. Danopoulos, G. Wilkinson, B. Hussain-Bates and M. B. Hursthouse, *J. Chem. Soc.*, *Dalton Trans.*, 1991, 1855.
40 G. M. Sheldrick, *Acta Crystallogr.*, *Sect. A*, 1990, **16**, 467.
41 G. M. Sheldrick, SHELXL, Program for Crystal Structure Refinement, University of Göttingen, 1993.